Journal of Power Sources 268 (2014) 171–175

Contents lists available at ScienceDirect

Journal of Power Sources

journal homepage: www.elsevier.com/locate/jpowsour

Short communication

Phosphorus-doped carbon nanotubes supported low Pt loading catalyst for the oxygen reduction reaction in acidic fuel cells

Ziwu Liu [a, b], Qianqian Shi [b], Rufan Zhang [c], Quande Wang [a], Guojun Kang [a], Feng Peng [b, *]

[a] Low Carbon Energy Institute, China University of Mining & Technology, Xuzhou 221008, Jiangsu, China
[b] Key Laboratory for Fuel Cell Technology of Guangdong Province, School of Chemistry and Chemical Engineering, South China University of Technology, Guangzhou 510640, China
[c] Beijing Key Laboratory of Green Chemical Reaction Engineering and Technology, Department of Chemical Engineering, Tsinghua University, Beijing 100084, China

HIGHLIGHTS

- 0.85% Pt supported on phosphorus-doped carbon nanotubes (Pt/P-CNTs) is designed.
- Pt/P-CNTs exhibit a high activity for oxygen reduction reaction in acidic media.
- The intrinsic activity and stability of Pt/P-CNTs are enhanced compared with Pt/CNTs.
- The enhanced performances are due to the strong interaction between Pt and P-CNTs.
- This strong Pt-support interaction is proven by experiment and theory calculations.

GRAPHICAL ABSTRACT

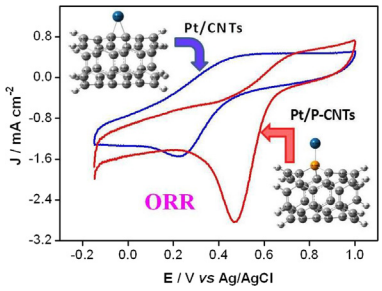

ARTICLE INFO

Article history:
Received 1 April 2014
Received in revised form
5 June 2014
Accepted 6 June 2014
Available online 16 June 2014

Keywords:
Fuel cells
Low platinum loading
Oxygen reduction reaction
Strong metal-support interaction

ABSTRACT

To develop low-cost and efficient cathode electrocatalysts for fuel cells in acidic media, phosphorus-doped carbon nanotubes (P-CNTs) supported low Pt loading catalyst (0.85% Pt) is designed. The as-prepared Pt/P-CNTs exhibit significantly enhanced electrocatalytic oxygen reduction reaction (ORR) activity and long-term stability due to the stronger interaction between Pt and P-CNTs, which is proven by X-ray photoelectron spectroscopic analysis and density functional theory calculations. Moreover, the as-prepared Pt/P-CNTs also display much better tolerance to methanol crossover effects, showing a good potential application for future proton exchange membrane fuel cell devices.

1. Introduction

One of the key challenges for commercialization of fuel cells is the cost of cathode platinum (Pt) catalysts [1]. To reduce the cost of cathode electrocatalysts, some approaches were taken over the past decades: (i) reducing Pt usage in Pt-based catalysts by coating Pt-monolayer shell on inexpensive metal nanoparticle cores [2] and

* Corresponding author. Tel./fax: +86 020 87114916.
E-mail address: cefpeng@scut.edu.cn (F. Peng).

http://dx.doi.org/10.1016/j.jpowsour.2014.06.036
0378-7753/

alloying Pt with other metals [3], (ii) replacing Pt catalyst with less expensive noble metal-based catalysts (Pd, Au, Ag, etc.) [4,5], (iii) developing non-precious metal-based electrocatalysts such as Fe–N or Co–N catalysts [6,7], and (iv) designing novel metal-free heteroatoms-doped carbon electrocatalysts, which emerged recently at the forefront of catalytic technologies for fuel cells [8–11]. Despite significant advances of the non-Pt catalysts mentioned above, the ORR performances of non-Pt catalysts are all inferior to those of Pt-based ones in terms of activity [8,12], especially in acidic conditions. At present, Pt-based catalysts are still the most active electrocatalysts towards the ORR [13], therefore, it will be the most effective strategy to design low Pt cathode catalysts with high performance in acid medium.

In our recent works, it was found that Pt/CNTs with low Pt loading (lower than 1 wt.%) exhibited good electrocatalytic activity toward the ORR and weak methanol oxidation activity in acidic medium [14,15], which could eliminate the effects of methanol crossover on cathode over potential of direct methanol fuel cells. However the ORR current density and onset potential of Pt/CNTs with low Pt loading are still very lower compared with the commercial Pt/C catalyst. To this end, it is of particular significance to know whether it is possible to design low Pt loading catalyst by the strong Pt-support interaction to improve the ORR activity. Herein, the phosphorus-doped carbon nanotubes (P-CNTs) were prepared and used as the support of low Pt loading catalyst to design low-cost ORR electrocatalyst in acidic medium. The results indicated that Pt/P-CNTs (0.85 wt.% Pt) displayed significantly improved electrocatalytic activity for the ORR and long-term stability due to the stronger interaction between Pt and P-CNTs, which was revealed by X-ray photoelectron spectroscopic (XPS) analysis and density functional theory (DFT) calculations.

2. Experimental section

The CNTs and P-CNTs were synthesized with the thermolysis method by utilizing toluene and triphenylphosphine (TPP) in accordance with the concentration of 0 and 10.0 wt.% of TPP in toluene solutions, respectively. The details were described in our recent paper [16]. Pt/CNTs and Pt/P-CNTs with the same Pt loadings (1.0 wt.% of theoretical loading) were prepared by the method of ethylene glycol reduction according to the Ref. [17]. The commercially available Pt–C (47.6 wt.% on Vulcan XC-72) catalyst was purchased from BASF Fuel Cell, Inc., USA.

The morphologies of the samples were characterized by scanning electron microscopy (SEM) (MERLIN compact) and high resolution transmission electron microscopy (HRTEM) (JEOL, JEM2010) operating at 200 kV. Elemental compositions of the P-doped CNTs were analyzed by Energy dispersive spectrometer (EDS) (S-3700N). XPS measurements were performed on a Thermo Scientific ESCALAB 250XI using Al Kα radiation.

Electrochemical experiments were carried out at room temperature in a three-electrode cell connected to an electrochemical analyzer (Eco Chemie B. V. Autolab PGSTAT30). The preparation of electrodes was described in our previous paper in detail [11]. The Cyclic voltammetry (CV) experiments were conducted in oxygen-saturated 1.0 M $HClO_4$ solutions at room temperature with the scan rate of 100 mV s^{-1}. Linear sweep voltammetry (LSV) measurements were performed in the oxygen-saturated 1.0 M $HClO_4$ solution at rotation rate of 1600 rpm with the scan rate of 10 mV s^{-1}. A glass carbon electrode coated catalyst was used as the working electrode, an Ag/AgCl with saturated KCl as reference electrode, and a Pt electrode (for LSV) or a graphite carbon (for CV) as counter electrode. All potentials were measured *vs*. the potential of Ag/AgCl electrode.

3. Results and discussion

Fig. 1(A) shows that Pt/P-CNTs display well-dispersed Pt nanoparticles compared to Pt/CNTs with some Pt agglomeration. The calculated average Pt particle sizes are 1.86 nm for Pt/P-CNTs and 2.30 nm for Pt/CNTs, meaning that P-CNT supports are in favor of the formation of smaller Pt nanoparticles. The immobilization of Pt on the surface of P-CNTs and CNTs was further confirmed by XPS analysis. As shown in Fig. 1(B), for the Pt/P-CNTs, double peaks with binding energy (BE) of 71.53 and 74.83 eV demonstrated the presence of metallic Pt, and the doublet near 72.13 and 75.4 eV could be assigned to Pt oxide. Meanwhile, it is noted that the BE of Pt 4f (71.53 and 74.83 eV) in Pt/P-CNTs is negatively shifted by 0.25 eV compared with that of Pt in Pt/CNTs (71.78 and 75.08 eV), indicating the existence of interaction between Pt and P-CNT supports [18]. The loading of Pt on the surface of Pt/P-CNTs and Pt/CNTs was measured to be about 0.85 wt.% by XPS. The P elemental content of 2.92 wt.% in P-CNTs bulk was probed by EDS. The successful doping of structural P was further confirmed by XPS. The content of phosphorus in P-CNTs surface is 0.76 wt.%, which is lower than that in P-CNTs bulk. Fig. 1(C) shows that the BE of P 2p (130.6 and 133.5 eV) in Pt/P-CNTs is positively shifted by 0.5–1.3 eV compared with that of P in P-CNTs (130.1 and 132.2 eV). Lower BE of Pt 4f and higher BE of P 2p in Pt/P-CNTs can be well explained by more negative charge distribution on Pt atoms and more positive charge distribution on P atoms due to the interaction between the Pt and P-CNTs.

The ORR catalytic activities of Pt/P-CNTs were investigated by the LSV compared with those of Pt/CNTs and commercial Pt/C catalysts. Fig. 2(A) shows that the onset of Pt/P-CNTs catalyst appearing at +0.81 V is much higher than that (at +0.65 V) of Pt/CNTs. Meanwhile, current densities of Pt/P-CNTs catalyst in the potential range of +0.6 to −0.15 V are not only much larger than those of Pt/CNTs but also larger than the current density sum of P-CNTs and Pt/CNTs, implying the synergistic effects between the P-CNT support and Pt. The diffusion-limited current of Pt/P-CNTs is 1.8 times that of Pt/CNTs. Considering to the effect of particle size, the surface-specific activity of Pt/P-CNTs is 1.5 times that of Pt/CNTs. These results indicate that the intrinsic electrocatalytic activity of low Pt loading catalyst for ORR has been significantly improved by the strong Pt-support interaction. Compared with the commercial Pt/C catalyst, the ORR current of Pt/P-CNTs is still lower than those of Pt/C, but the mass-specific current of Pt (4860 A g^{-1} at 0 V) in Pt/P-CNTs is fifty times larger than that of Pt in Pt/C (96 A g^{-1} at 0 V), further demonstrating the remarkable improvement of the ORR activity of Pt loading on the P-CNTs support.

For a better understanding of the observed electrocatalytic activity of Pt/P-CNTs for the ORR, the CV was employed to further estimate the ORR activity. In Fig. 2(B-20) and (C-20), it is obvious that the ORR peak potential at about +0.46 V and the peak current density of 2.72 mA cm^{-2} for Pt/P-CNTs are all much higher than those (about +0.25 V, 1.55 mA cm^{-2}) for Pt/CNTs, confirming the significant improvement of ORR activity of low Pt loading on the P-CNTs surface, which is almost agreement with the data from the LSV measurement. These results demonstrate that the Pt/P-CNTs catalyst displays significantly improved electrocatalytic activity for the ORR without the rotation of cathode electrode in practical application. For the Pt/CNTs catalyst, the loss of the peak current was about 69.6% only after 1000 cycles, and the peak current almost disappeared after 2000 cycles (Fig. 2(B)). The loss of the peak current of the commercial Pt/C was about 79.6% after 3000 cycles (Fig. 2(C)). In contrast, the peak current of Pt/P-CNTs just lost 63.5% after 3000 cycles and the peak current disappeared after 5000 cycles (Fig. 2(D)), indicating the longer-term stability of Pt/P-CNTs than those of Pt/CNTs and commercial Pt/C due to the strong

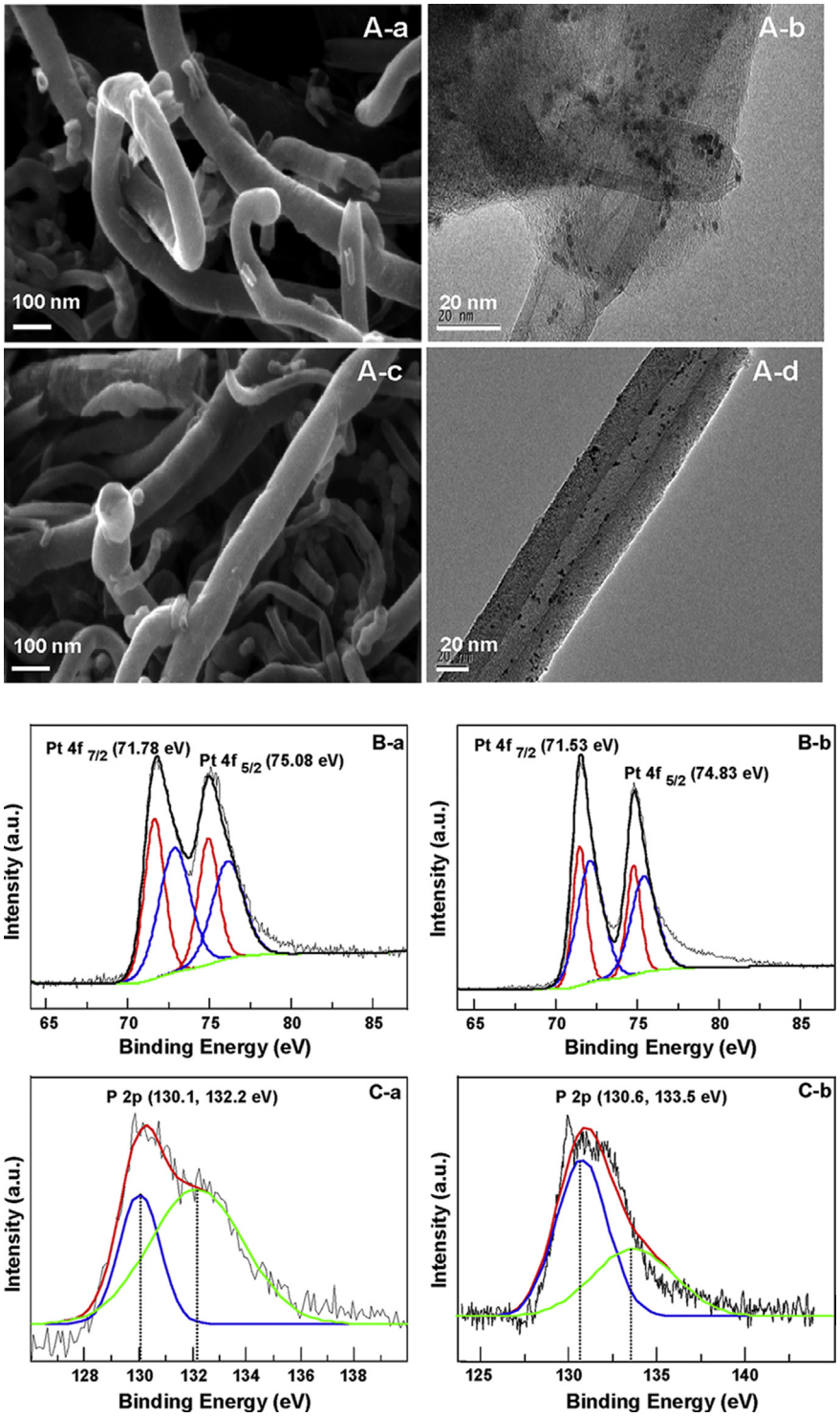

Fig. 1. SEM and TEM images of the Pt/CNTs (A-a, A-b) and Pt/P-CNTs (A-c, A-d). XPS spectra of Pt 4f for the Pt/CNTs (B-a) and Pt/P-CNTs (B-b). XPS spectra of P 2p for the P-CNTs (C-a) and Pt/P-CNTs (C-b).

interaction between Pt and P-CNTs support. The tolerance to methanol crossover effects was determined by the CV in an oxygen-saturated 1.0 M $HClO_4$ solution containing 1.0 M CH_3OH. It is interesting to note that no evident methanol oxidation peak appeared for Pt/P-CNTs, and the ORR performance is almost the same in 1.0 M $HClO_4$ solution with and without methanol (Fig. 2(E)). But for the commercial Pt/C catalyst, the ORR peak at about +0.62 V absolutely disappeared when methanol oxidation peak arose at about +0.73 V (Fig. 2(F)), confirming that the low Pt loading catalyst has much high ORR activity and weak methanol oxidation activity, showing a remarkably good resistance to methanol.

Encouraged by the outstanding electrochemical properties of the Pt/P-CNTs with ultra-low Pt loading in acidic medium, DFT calculations were performed to understand the advantages of Pt/P-CNTs compared to Pt/CNTs for the first time. All calculations were

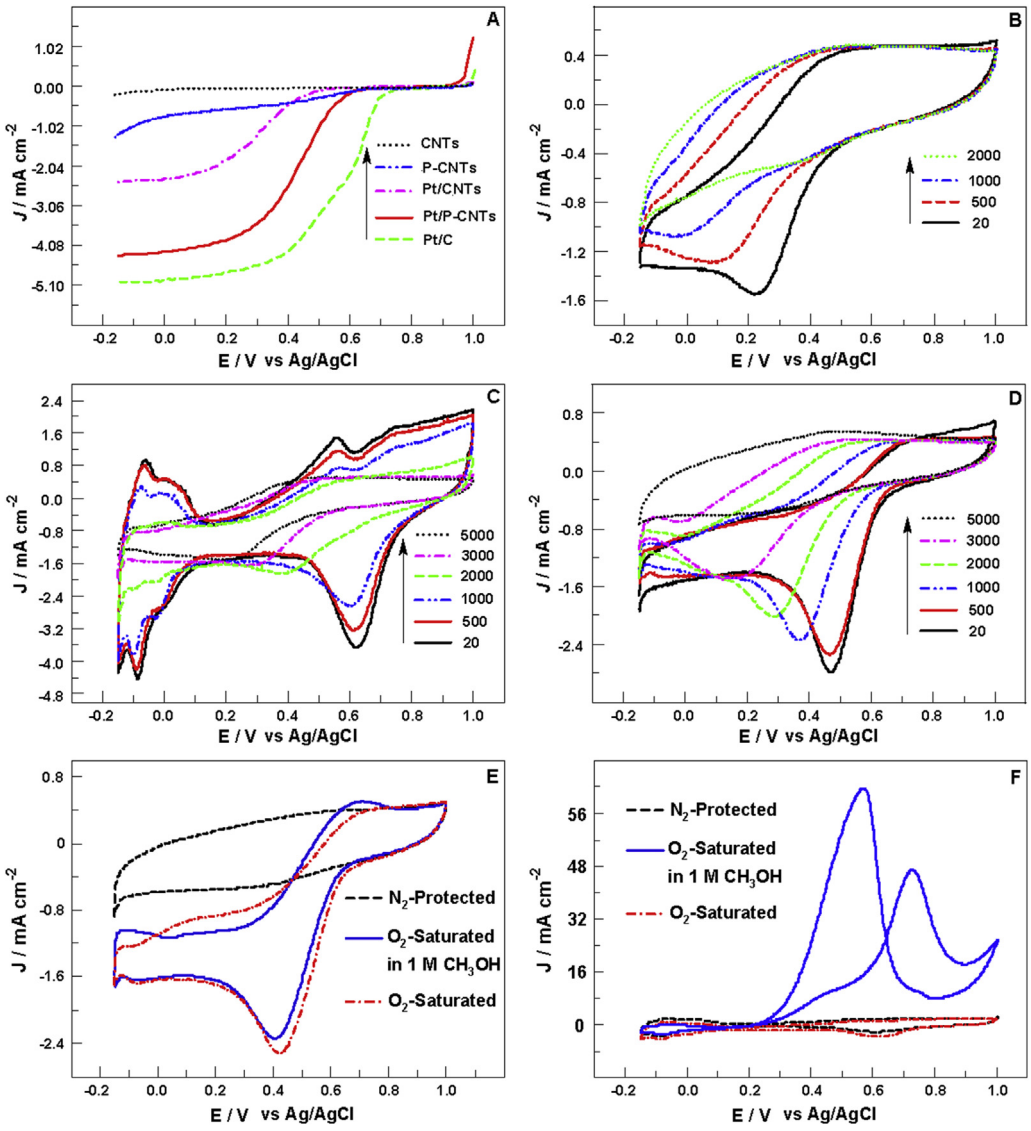

Fig. 2. LSV curves (A) at 1600 rpm in the oxygen-saturated 1.0 M $HClO_4$ solution with oxygen flow rate of 50 mL min^{-1} and scan rate of 10 mV s^{-1}. CV curves recorded during the repeated cycling for the Pt/CNTs (B), Pt/C (C) and Pt/P-CNTs (D) in an oxygen-saturate1.0 M $HClO_4$ solution, and CV curves for the Pt/P-CNTs (E), and Pt/C (F) in a nitrogen-protected or an oxygen-saturated 1.0 M $HClO_4$ solution, and in an oxygen-saturated 1.0 M $HClO_4$ solution upon addition of CH_3OH (1.0 M) with oxygen flow rate 20 mL min^{-1} and scan rate of 100 mV s^{-1}.

performed by using the Gaussian 09 program, and the B3LYP density functional, i.e., Becke's three-parameter nonlocal exchange functional with the nonlocal correlation functional of Lee, Yang, and Parr [19] have been employed. The 6-31G (d, p) basis set has been used for C, P, and H atoms, while Pt atom is described by the LANL2DZ basis set including a double-valence basis set with the Hay and Wadt effective core potential [20]. The binding energy is calculated employing the following expression: $E_b = E$ (Pt/CNT or P-CNT) − E (CNT or P-CNT) − E (Pt), where E (Pt/CNT or P-CNT), E (CNT or P-CNT) and E (Pt) denote the total energies of the optimized Pt binding on CNT or P-doped CNT, the CNT or P-doped CNT, and a single Pt atom, respectively. Fig. 3 illustrates the stable geometries of single Pt atom on the intrinsic CNT surface (Fig. 3(A)) and on the different adsorption sites of P-doped CNT (Fig. 3(B)–(D)), while Table 1 gives the corresponding binding energy and Mulliken charge of Pt atom.

It can be seen that the binding energies of single Pt atom loaded on both CNT and P-CNT supports are all much greater than van der Waals interaction, demonstrating that the adsorption modes of Pt atom on two supports are all chemisorptions as the quantum chemistry calculation results of Pt atom supported on nitrogen-doped and boron-doped CNTs [21]. Among the three optimized configurations of Pt atom binding on different positions of P-CNT support, the Pt/P-CNT (B) structure is the most stable configuration and the Pt/P-CNT (C) is the most unstable one because of the effect of steric hindrance. The convex P atom in P-CNT network facilitates the loading of Pt atom and the cupped neighboring C atoms in P-CNT space structure does not favor the Pt atom loading relatively. Compared to the binding energy of Pt atom on pure CNT surface, the binding energies of Pt atom in Pt/P-CNT (B) and Pt/P-CNT (D) structures are much larger, which may lead to the enhanced stability of Pt on P-CNT support directly. Meanwhile, it is worth noting that the electron densities of Pt atom on P-CNTs (B and D) are more negative than those on the pure CNT surface (Table 1), especially, in the most stable P-CNT (B) configuration. Similarly, the electron densities of P atom are more positive after supporting Pt, revealing that the bonding electrons between Pt—P or Pt—C bond tend to distribute on Pt atom in Pt/P-CNT optimized structures because of

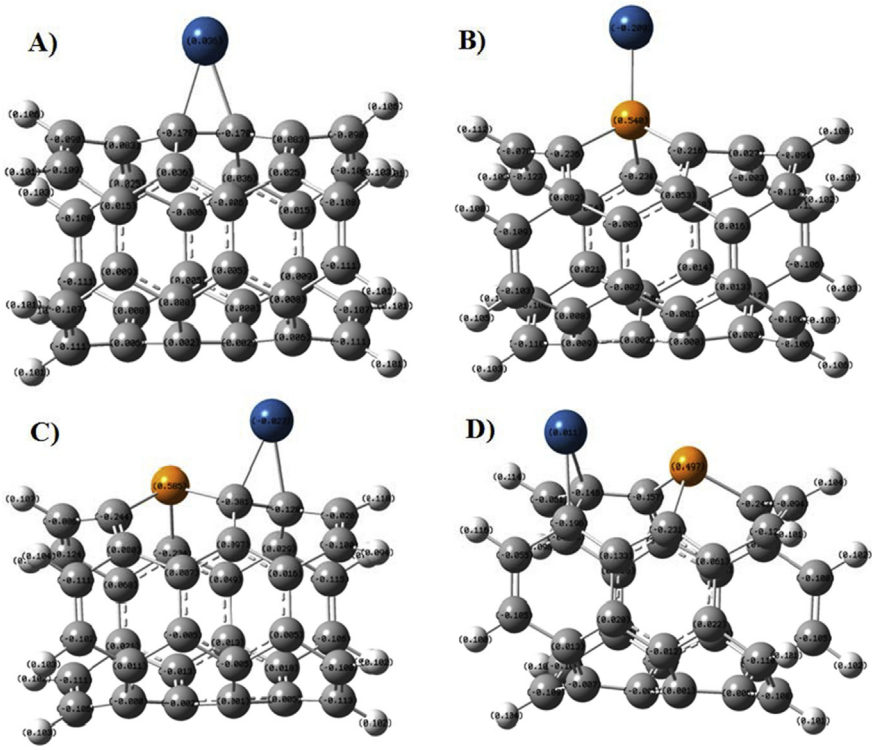

Fig. 3. The optimized configurations of single Pt atom binding on the intrinsic CNT surface (A) and different adsorption sites of P-CNTs (B, C, D). Gray: C atom, orange: P atom, blue: Pt atom. (For interpretation of the references to color in this figure legend, the reader is referred to the web version of this article.)

the donor electron properties of P atom. These results are in good agreement with the analyses of XPS, that is, lower BE of Pt 4f and higher BE of P 2p in Pt/P-CNTs. The great alteration of electron densities of Pt atom on P-CNT support may be the direct reason for the significant ORR activity improvement of Pt/P-CNTs. In addition, phosphorus doping could have an effect on the conductivity of CNTs. In our previous report [22], the result of the electrochemical impedance spectroscopy measurement showed that charge transfer at the P-CNTs/electrolyte interface would encounter smaller resistance, which could facilitate the kinetics of ORR.

4. Conclusions

P-CNTs could be used as support of low Pt loading catalyst to design low-cost ORR electrocatalyst in acidic medium. The as-prepared Pt/P-CNTs (0.85% Pt) exhibited significantly enhanced electrocatalytic ORR activity and long-term stability due to the stronger interaction between Pt and P-CNTs, which was proven by XPS analysis and DFT calculations. Moreover, the Pt/P-CNTs also exhibited much better tolerance to methanol than the commercial Pt/C catalyst. These results show a good potential for the designing of low-cost and efficient ORR catalysts.

Table 1
Binding energy and charge distribution of single Pt atom supported on the CNT surface and different adsorption sites of P-CNT supports, and the charge distribution of P atom in P-CNT supports.

Configurations	E_b (kcal mol^{-1})	Pt charge distribution[a]	P charge distribution[a]
P-CNTs	–	–	0.455
Pt/CNT (A)	49.80	0.036	–
Pt/P-CNT (B)	59.00	−0.209	0.540
Pt/P-CNT (C)	40.01	−0.027	0.585
Pt/P-CNT (D)	55.34	0.011	0.497

[a] Mulliken Charge distribution.

Acknowledgments

Financial supports from National Science Foundation of China (No. 21376257), the Jiangsu Provincial Natural Science Foundation of China (No. BK20131112), and the Open Projects of Key Laboratories for Green Chemical Product and Fuel Cell Technologies of Guangdong Province (No. GC201201) are greatly acknowledged.

References

[1] M.K. Debe, Nature 486 (2012) 43–51.
[2] H.I. Karan, K. Sasaki, K. Kuttiyiel, C.A. Farberow, M. Mavrikakis, R.R. Adzic, ACS Catal. 2 (2012) 817–824.
[3] J.B. Wu, J.L. Zhang, Z.M. Peng, S.C. Yang, F.T. Wagner, H. Yang, J. Am. Chem. Soc. 132 (2010) 4984–4985.
[4] L. Zhang, F. Hou, Y.W. Tan, Chem. Commun. 48 (2012) 7152–7154.
[5] Y. Song, K. Liu, S.W. Chen, Langmuir 28 (2012) 17143–17152.
[6] G. Wu, K.L. More, C.M. Johnston, P. Zelenay, Science 332 (2011) 443–447.
[7] M. Lefevre, E. Proietti, F. Jaouen, J.-P. Dodelet, Science 324 (2009) 71–74.
[8] Y.G. Li, W. Zhou, H.L. Wang, L.M. Xie, Y.Y. Liang, F. Wei, J.C. Idrobo, S.J. Pennycook, H.J. Dai, Nat. Nanotechnol. 7 (2012) 394–400.
[9] Z. Yang, H.G. Nie, X.A. Chen, X.H. Chen, S.M. Huang, J. Power Sources 236 (2013) 238–249.
[10] X.M. Zhou, Z. Yang, H.G. Nie, Z. Yao, L.J. Zhang, S.M. Huang, J. Power Sources 196 (2011) 9970–9974.
[11] Z.W. Liu, F. Peng, H.J. Wang, H. Yu, W.X. Zheng, J. Yang, Angew. Chem. Int. Ed. 50 (2011) 3257–3261.
[12] Z.W. Chen, D. Higgins, A.P. Yu, L. Zhang, J.J. Zhang, Energy Environ. Sci. 4 (2011) 3167–3192.
[13] N.A. Karim, S.K. Kamarudin, Appl. Energy 103 (2013) 212–220.
[14] Z.W. Liu, F. Peng, H.J. Wang, H. Yu, C.L. Chen, Q.Q. Shi, Catal. Commun. 29 (2012) 11–14.
[15] X. Li, H.J. Wang, H. Yu, Z.W. Liu, F. Peng, J. Power Sources 260 (2014) 1–5.
[16] Z.W. Liu, F. Peng, H.J. Wang, H. Yu, J. Tan, L.L. Zhu, Catal. Commun. 16 (2011) 35–38.
[17] C.M. Zhou, F. Peng, H.J. Wang, H. Yu, C. Peng, J. Yang, Electrochem. Commun. 12 (2010) 1210–1213.
[18] G. Wu, D. Li, C. Dai, D. Wang, N. Li, Langmuir 24 (2008) 3566–3575.
[19] W. Yang, R.G. Parr, C. Lee, Phys. Rev. A 34 (1986) 4586–4590.
[20] P.J. Hay, W.R. Wadt, J. Chem. Phys. 82 (1985) 270–283.
[21] Y.H. Li, T.H. Hung, C.W. Chen, Carbon 47 (2009) 850–855.
[22] Z.W. Liu, Q.Q. Shi, F. Peng, H.J. Wang, H. Yu, J.C. Li, X.Y. Wei, Catal. Commun. 22 (2012) 34–38.